

# **STUDY OF HIGHER NON-PRECIOUS METAL LOADINGS IN OXYGEN REDUCTION CATALYSTS FOR USE IN PROTON EXCHANGE MEMBRANE FUEL CELL**

HONORS THESIS

Presented in Partial Fulfillment of the Requirements for Graduation with Distinction in  
the Degree Bachelor's of Science at The Ohio State University

By

Daniel J. Valco

\* \* \* \* \*

The Ohio State University  
Department of Chemical and Biomolecular Engineering  
2011

Honors Thesis Committee:

Professor Umit S. Ozkan, Adviser

Professor James Rathman



## **ABSTRACT**

The effect of higher non-precious metal loading in oxygen reduction catalysts for use in proton exchange membrane fuel cell catalysts was investigated using the rotating ring disk electrode and rotating disk electrode methods. Metal loadings of 6, 10, and 15 weight percent were deposited on a support where acetonitrile decomposition in an inert atmosphere formed a carbon-nitride material that was active for the electroreduction of oxygen in an acidic medium. Activity results indicate that higher metal loading in the carbon growth media affects the activity of oxygen reduction catalysts formed during carbon growth. These iron phases and oxidation states of the growth media was further characterized during in-situ pyrolytic carbon growth using X-ray absorption techniques. It was found that the iron phase of the impregnated support mostly consisted of mixed oxides, which were reduced to metallic iron and iron carbide upon the introduction of acetonitrile that caused carbon growth.

## ACKNOWLEDGMENTS

I would like to thank my adviser, Dr. Umit S. Ozkan, for the opportunity to participate in undergraduate research and challenging me to pursue this thesis.

I thank Deepika Singh for intellectual support, patience in teaching me catalyst preparation and testing, guidance throughout my year of research, and for encouragement throughout the process of completing this thesis. I also thank her for assistance with catalyst preparation and providing data and information on XANES for this document.

I thank Dieter von Deak for intellectual support and his assistance in the laboratory when Deepika was unavailable.

I also appreciate Jesaiah King for his help in the lab with preparation of catalysts that are discussed in this thesis.

This research was supported by financial support for this work from US Department of Energy Basic Energy Sciences through the grant DE-FG02-07ER15896. Portions of this work were performed at the DuPont-Northwestern-Dow Collaborative Access Team (DND-CAT) located at Sector 5 of the Advanced Photon Source (APS). DND-CAT is supported by E.I. DuPont de Nemours & Co., The Dow Chemical Company and the State of Illinois. Use of the APS was supported by the U. S. Department of Energy, Office of Science, Office of Basic Energy Sciences, under Contract No. DE-AC02-06CH11357. The author also acknowledges the NSF support for acquisition of the XPS system under NSF-DMR grant #0114098.

## TABLE OF CONTENTS

<b>ABSTRACT</b> .....	i
<b>ACKNOWLEDGMENTS</b> .....	ii
<b>LIST OF TABLES</b> .....	iv
<b>LIST OF FIGURES</b> .....	v
<b>INTRODUCTION</b> .....	1
<b>EXPERIMENTAL METHODS</b> .....	4
<i>Catalyst Synthesis</i> .....	4
<i>Catalyst Testing</i> .....	6
<i>Rotating Ring Disk Electrode (RRDE) Testing</i> .....	7
<i>Rotating Disk Electrode (RDE) Testing</i> .....	8
<i>X-Ray Absorption Near Edge Spectroscopy (XANES) Analysis</i> .....	8
<b>RESULTS AND DISCUSSION</b> .....	12
<i>Catalysts</i> .....	12
<i>Catalysts Grown over Magnesium Oxide Supports</i> .....	13
<i>Catalysts Grown over Vulcan Carbon Supports</i> .....	17
<b>CONCLUSIONS</b> .....	21
<b>FUTURE WORK</b> .....	22

## LIST OF TABLES

Table 1: Metal Loadings of Catalysts Prepared.....	12
--	----

## LIST OF FIGURES

Figure 1: Diagram of PEM Fuel Cell Operation Image.....	2
Figure 2: Excitation of a Core Electron in XAFS.....	9
Figure 3: Experimental Setup of XANES at Argonne National Laboratory .....	11
Figure 4: RDE Activity Comparison of Catalysts Prepared Using MgO Support .....	13
Figure 5: RRDE Activity Comparison of Catalysts Prepared Using MgO Support.....	15
Figure 6: Complete Absorption Spectra of 6 weight percent Fe-MgO.....	16
Figure 7: Percentage Composition of Iron Oxides in MgO samples .....	17
Figure 8: RRDE Activity Comparison of Catalysts Prepared Using VC Support.....	18
Figure 9: Complete Absorption Spectra of 6 weight percent Fe-VC.....	19
Figure 10: Percentage Composition of Iron Oxides in VC sample .....	20

## INTRODUCTION

Proton exchange membrane (PEM) fuel cells are attractive energy conversion devices that convert hydrogen and oxygen fuels to water via a zero-emission process. The fuel cell has potential for application in power generation for vehicles, which can help alleviate society's reliance on fossil fuels. A PEM fuel cell consists of an anode, an electrolyte, a cathode, and catalyst. The anode is the negatively charged side of the fuel cell and conducts the electrons that are removed from the hydrogen fuel to be used for power generation in an external circuit. The electrolyte in a PEM fuel cell is a sulfonated tetrafluoroethylene based fluoropolymer-copolymer membrane, which repels electrons and attracts the positively charged hydrogen ions. The membrane forces the electrons to flow through the external circuit, while allowing the positively charged protons to pass through the membrane from the anode to the cathode. The cathode is the positively charged side of the fuel cell and consumes electrons from the external circuit in an electrocatalytic reaction between protons and oxygen to form into water. The catalyst is a porous, high surface area material that varies on the anode and cathode side of the fuel cell.

The fuel cell operates using two gases, one hydrogen fuel and the other atmospheric oxygen. The hydrogen gas is flowed to the anode side of the fuel cell, where the anode catalyst oxidizes hydrogen ( $H_2$ ) to produce two electrons and two protons.



The electrons travel through an external circuit to generate power, while the hydrogen ions diffuse through the fuel cell membrane to the cathode due to a concentration gradient. Meanwhile, oxygen is flowed over the cathode side where the cathode catalyst reduces oxygen (O<sub>2</sub>) in the presence of protons and 4 electrons to produce water (H<sub>2</sub>O) and complete the circuit. A picture of the process can be seen in Figure 1 below.

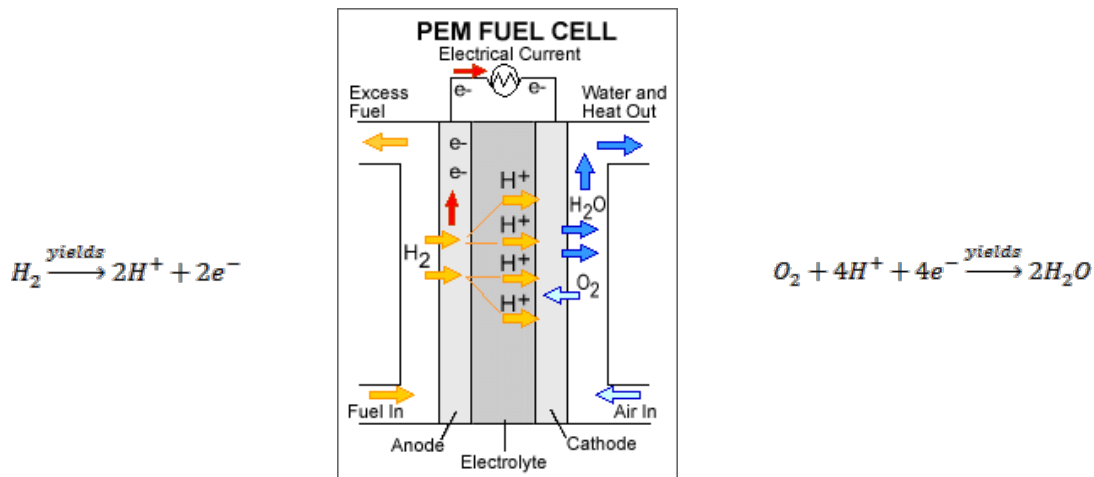
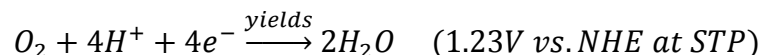


Figure 1: Diagram of PEM Fuel Cell Operation Image  
 Image Courtesy of the United States Department of Energy  
[http://www1.eere.energy.gov/hydrogenandfuelcells/fuelcells/fc\\_types.html#pem](http://www1.eere.energy.gov/hydrogenandfuelcells/fuelcells/fc_types.html#pem)

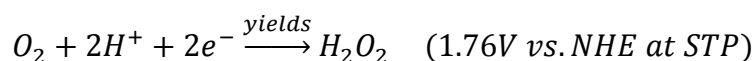
A major roadblock in commercializing cathode hydrogen fuel cell technology is the high cost and scarcity of the platinum catalysts that are currently used as the industry standard, specifically high platinum loadings at the cathode are needed to overcome the high overpotential of the oxygen reduction reaction (ORR). The desired 4-electron transfer reaction to form water, even with a state-of-the-art platinum catalyst is relatively slow and requires a large overpotential to increase the kinetics, thereby decreasing the power and efficiency of the fuel cell [1]. Therefore, research on non-precious metal carbon-based ORR catalysts is being conducted in order to improve the issues associated with the cathode catalyst in hopes of making PEM fuel cell commercialization a reality.

Initial studies of ORR carbon-nitrogen catalysts were conducted by Jasinski using macrocycles in the 1960s. Jasinski's work focused on ORR catalysts that adsorb oxygen reversibly without degradation of the catalytically active nitrogen coordinated metal active site by using porphyrins and the metal phthalocyanines [2-3]. These molecules were chosen since a similar active site is present in hemoglobin, which adsorbs oxygen on an active iron site stabilized by nitrogen groups of the macrocycles [2-3]. Although macrocycles were active for ORR, the rapid degradation of the catalyst in acidic environments made them unstable in a fuel cell environment [4]. However, high temperature treatment of these macrocycles under an inert atmosphere was found to increase the stability, while maintaining catalytic performance [4-5]. Studies of these macrocycle catalysts have laid the foundation for ORR catalyst research. Current work on non-precious metal ORR catalysts focuses on nitrogen-coordinated iron in a carbon matrix (Fe/N/C) [6]. The most active non-precious metal catalysts prepared with Fe/N/C are approaching performance levels similar to state-of-the-art platinum carbon (Pt/C) catalysts used in PEM fuel cells [7]. As a result, the Fe/N/C catalysts are attractive candidates for mitigating the high costs associated with Pt/C catalysts [8].

The Fe/N/C catalyst research within this thesis focuses on the ORR catalysts at the cathode of the PEM fuel cell. The two main reactions that can take place at the cathode of the fuel cell are the desired 4-electron transfer to water



and the undesired 2-electron transfer to hydrogen peroxide.



Due to the unknown nature of the mechanism by which oxygen reduction occurs on the cathode, it is essential to analyze the role of iron and its effects on catalyst activity. However, much ambiguity exists about the role iron plays in the activity of a catalyst. Some researchers believe that iron is stabilized by the formation of pyridinic nitrogen groups located at the edge plane of the carbon, allowing iron to act as the active site [9]. On the other hand, some researchers are of the opinion that iron is not part of the active site but acts as a catalyst for the formation of the oxygen reduction active site [1]. By modifying iron loadings in growth media during the formation of the carbon-nitrogen graphite oxygen reduction catalyst, a correlation with activity and the iron content could be determined; thereby allowing a conclusion to whether or not higher iron content helps or inhibits catalyst activity. The hypothesis for the thesis is that higher iron content will inhibit the catalyst activity. This study will further the understanding of the role that iron plays in the oxygen reduction reaction in PEM fuel cell catalysts via activity tests using a Rotating Disk Electrode (RDE), Rotating Ring Disk Electrode (RRDE), and X-ray Absorption Near Edge Structure (XANES).

## **EXPERIMENTAL METHODS**

### ***Catalyst Synthesis***

Catalysts were prepared using an incipient wetness impregnation technique. Incipient wetness impregnation (IWI) is a process where an acetate salt is dissolved in a solvent and then impregnated into the pore volume of a high surface area catalytic support. The growth medias are prepared by mechanically mixing iron (II) acetate into a

high surface area (HSA) support that was either nanoparticle-sized magnesia (MgO) or Vulcan carbon (VC). The metal impregnated or doped growth media is dried at 110°C overnight in a drying oven. The metal iron loadings investigated were 6, 10, and 15 weight percent. In order to accomplish the various metal loadings, the amount of iron (II) acetate impregnated into the support was increased. For the higher metal loadings (10% and 15%), the IWI was performed in two impregnation steps where a portion of the loading was added to the high surface area support and then allowed to dry. After drying, the remainder of the loading was impregnated and growth media was dried again.

After drying, acetonitrile ( $\text{CH}_3\text{CN}$ ) is decomposed over the metal impregnated growth media under pyrolysis conditions to form graphitic carbon nitride. Pyrolysis is a heat treatment at high temperatures without the presence of oxygen, which allows for the decomposition of organic materials and formation of carbon deposits. To synthesize the  $\text{CN}_x$  catalyst, the IWI support media was loaded into a quartz tube, which is placed into a pyrolysis furnace that is heated to 800°C in an inert nitrogen atmosphere. Once the desired carbon growth temperature was reached, acetonitrile gas was flowed over the catalyst for 2 hours using a room temperature bubbler where 150 ml/min of nitrogen was passed through. This process allows the formation of nitrogen doped carbon nanostructures ( $\text{CN}_x$ ) on the growth media. The inclusion of nitrogen in the graphitic carbon matrix helps achieve essential properties for high electronic conductivity, corrosion resistance, surface properties, while providing a low cost oxygen reduction PEM fuel cell catalyst [10]. In addition, high temperature pyrolysis improves the stability of the catalyst, as well as the catalytic activity [11]. After the completion of the

acetonitrile process, the catalyst is cooled to room temperature under nitrogen environment.

After pyrolysis, the resulting  $CN_x$  catalyst was acid treated in 1M hydrochloric acid (HCl) solution for 1 hour at 60°C. The catalyst was then rinsed with deionized (DI) water and allowed to dry in an oven. The acid treatment removes the non-electrically conducting oxide support and any exposed metal particles, in order to enhance catalyst activity. Once dried, the catalyst was tested for oxygen reduction activity using electrochemical half-cell techniques.

### ***Catalyst Testing***

The catalysts were evaluated for oxygen reduction activity using an electrochemical cyclic voltammetric technique, which can evaluate the catalyst's ORR activity and/or selectivity in two different half-cell environments: one argon enriched and another oxygen enriched. First, the catalyst ink used for testing has a composition of 1:10:160 (by mass) catalyst: 5% Nafion in aliphatic alcohols: ethanol. The ink solution was sonicated for thirty minutes prior to application to the test electrode, to insure relatively uniform dispersion of the catalyst in the ink solution. Next, cyclic voltammetry tests were performed to determine the capacitive current of the ORR-active  $CN_x$ . Cyclic voltammograms in oxygen and argon are conducted in a 0.5M sulfuric acid ( $H_2SO_4$ ) solution using an Ag/AgCl reference electrode and a Pt wire counter electrode. The two devices used to obtain the ORR information are a Rotating Disk Electrode (RDE) and a Rotating Ring Disk Electrode (RRDE). All potentials reported in this paper are referenced relative to the normal hydrogen electrode (NHE).

### *Rotating Ring Disk Electrode (RRDE) Testing*

The RRDE system used was connected to a Pine Instruments RRDE accessory fitted with a Pine MT28 tip fitted with a glassy carbon disk and platinum ring. Three 5  $\mu\text{L}$  aliquots of ink were applied to the 0.1642  $\text{cm}^2$  glassy carbon, resulting in a catalyst loading of 426  $\mu\text{g}/\text{cm}^2$ . A Bistat from Biologic Instruments controlled the electrochemical potential and measure the currents created.

RRDE testing begins in an oxygen saturated electrolyte. A single cyclic voltammogram (CV) scans at 10 mV/s from 1.2V to 0V to 1.2V vs. NHE. The purpose of this initial scan was to remove bubbles, thereby fully wetting the catalyst to insure the Bistat is accurately reading the potentials. Once completed, argon was diffused into the half-cell to displace the oxygen. An argon background scan is then conducted in a two-step process. The first step was 10 consecutive CVs from 1.2V to 0V to 1.2V vs. NHE at a rate of 50 mV/s to insure all contaminants and oxygen are removed from the electrode; thereby stabilizing the CV and cleaning the catalyst electrode surface. Next, a Faradaic capacitance scan for the disk was obtained by scanning from 1.2V to 0V to 1.2V vs. NHE at a rate of 10 mV/s in the argon-saturated acid electrolyte under a rotation of 100 rpm. Simultaneously, a background for the ring is obtained by holding the ring at 1.2V vs. NHE. The half-cell solution is then sparged with oxygen to allow study of the catalyst's oxygen reduction selectivity and activity. Once saturated, a similar process was conducted in the oxygen environment as done previously in the argon-saturated solution. A stability scan in the oxygen environment is conducted (ten consecutive CVs from 1.2V to 0V to 1.2V vs. NHE at a rate of 50 mV/s). A CV at a rotation of 100 rpm was then scanned from 1.2V to 0V to 1.2V vs. NHE at a rate of 10 mV/s on the catalyst coated

disk electrode. The ring was held at a constant 1.2V vs. NHE concurrently with the CV on the disk. Identical CVs were repeated at rotation rates of 0 rpm and 1000 rpm. The argon background scan was subtracted from the three oxygen CVs at different rotation rates. It should be noted prior to each step requiring a potential hold on the ring; the ring was conditioned by scanning from 0.2V to 1.8V to 0.2V vs. NHE at 100 mV/s for 20 scans.

#### *Rotating Disk Electrode (RDE) Testing*

A RDE system used was connected to a Princeton Applied Research (PAR) model 636 RDE accessory fitted with a Pine MT28 tip fitted with a glassy carbon disk electrode. Two aliquots of catalyst ink with same aforementioned composition, one of 5.5  $\mu\text{L}$  and another 6  $\mu\text{L}$  were applied to the 0.1256  $\text{cm}^2$  glassy carbon disk electrode, resulting in a catalyst loading of 426  $\mu\text{g}/\text{cm}^2$ . A Bistat from Biologic Instruments controlled the electrochemical potential and monitored the current produced. The RDE testing is identical to the aforementioned RRDE process; except that no ring scans can be conducted using this setup. Therefore, no selectivity information was compiled for catalysts tested using the RDE.

#### *X-Ray Absorption Near Edge Spectroscopy (XANES) Analysis*

X-Ray Absorption Fine Structure (XAFS) provides detailed information about the chemical composition and local bonding structure of a particular element in a compound. The technique is based on the absorption of X-rays by an atom, and the creation of photoelectrons, which are either excited to holes in the valence levels, or to unbound states and scattered by nearby atoms in a lattice; see Figure 2. The X-ray absorption spectrum shows edges corresponding to the binding energy of electron core levels in the

atom. On the other hand, if the atom is bound to other atoms in a lattice, the absorption edge jump varies significantly because of its local coordination states.

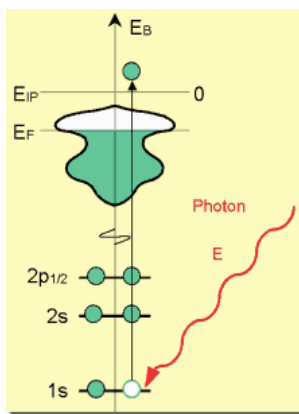


**Figure 2: Excitation of a Core Electron in XAFS**  
Image Courtesy of <http://home.postech.ac.kr/~chey/xafs-explain.htm>

This thesis will focus chiefly on X-ray absorption near edge spectroscopy (XANES). XANES is applicable to only the absorption edge jump and is very sensitive to the valence state of the atom and its bonding geometry. This technique, however, is a bulk technique and lacks surface sensitivity, but is useful for supported catalysts where one is interested in the composition of the entire particle.

XANES is based on the absorption of an X-ray photon which excites an electron from a core level (e.g.,  $1s$  or  $2p_{3/2}$ ) to an unoccupied state close to the Fermi level. This corresponds to the sharp edge jump seen at known energies for specific elements of the periodic table. The edge position corresponds to the ionization threshold, and thus reflects the oxidation state of the atom. At energies above the edge, core electrons are excited to continuum states and the spectra becomes dominated by a scattering wave-like phenomenon. As a result, the shape of the XANES spectrum depends straightforwardly on the states available to the excited electron. These depend on several factors such as



coordination of the atom, its mode of bonding and oxidation states, which imparts a greater degree of chemical sensitivity to XANES.

Iron K-edge XANES spectra was obtained at Sector 5 BM-D Advanced Photon Source of Argonne National Laboratory. The setup consisted of a high temperature carbolite furnace aligned in the beam path for X-ray transmission. A quartz reactor with an outer diameter of 1 cm was placed in a quartz tube attached to vacuum fittings on the sides to maintain a leak-proof environment within the tube. The tube was aligned with the beam such that the beam was in line with the  $CN_x$  growth pellets placed in the quartz reactors. The quartz reactor was attached to a temperature controller with an upper limit of 800°C, which was the primary reason for the choice of pyrolysis temperature for catalyst growth to be set at 800°C.

Pellets were prepared for use in the XANES. The pellets must be homogeneous and uniformly thin for x-rays to pass through them such that there is little discontinuity in the thickness or concentration of the concerned metal in the sample, which may lead to abnormalities in the x-ray absorption edge jump. The substrate concentration in the pellet was determined by the XAFSMASS software, which is in the order of ~10 mg for Fe-based substrates. For the pellet formation, 10-15 mg was Fe-MgO or Fe-VC substrate was ground using an agate mortar and pestle and pressed into a self supporting pellet. This was then inserted in a quartz reactor, which was placed in the quartz boat and then in the furnace pictured in Figure 3.

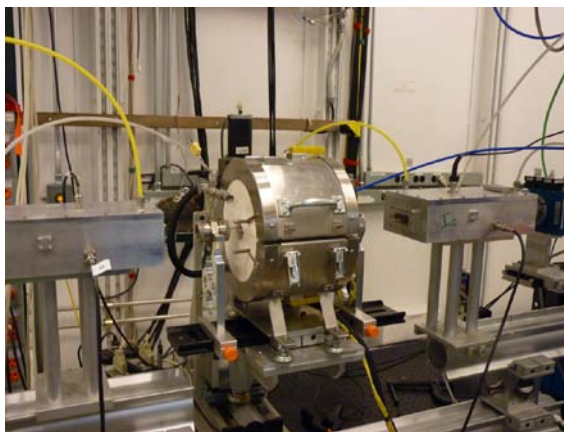


**Figure 3: Experimental Setup at Sector 5 BM-D, Advanced Photon Source, Argonne National Laboratory**

The first scan for XANES was taken at room temperature under the flow of nitrogen. The quartz reactor was then purged with 30 ml/min nitrogen for 30 minutes before ramping up the temperature to 800°C at 20°C/min. Once the temperature reached 800°C, another X-ray scan was collected before the introduction of acetonitrile. Subsequent scans were collected at 30, 60, 90 and 120 minutes under flow of acetonitrile. The same scanning procedure was used for all the growth catalysts.

The XANES spectra collected at different reaction times was compared with the XANES from known available standards such as  $\text{Fe}_2\text{O}_3$ ,  $\text{FeO}$ ,  $\text{Fe}_3\text{O}_4$ ,  $\text{FeC}$ , and  $\text{Fe}$  foil. A XANES fit for was performed on each spectrum to obtain a relative percentage composition of each known standard in the sample. The previously used 2 weight percent iron doped support samples had lower concentrations of Fe than desired in XAFS analysis, making the edge jump obtained extremely small and a low subsequent signal to noise ratio. As a result, higher loadings of iron were impregnated on the supports so that appropriate X-Ray absorption analysis could be conducted.

## RESULTS AND DISCUSSION

### *Catalysts*

This paper investigates the effects of higher non-precious metal loading in catalysts for use in a PEM fuel cell. The catalysts studied were impregnated with an iron salt prior to acetonitrile pyrolysis at 800°C. Two major carbon-nitride growth factors were studied in this thesis; the loading of iron in the carbon growth media, and type of the iron present in the support that used for carbon growth. In this case, either magnesia or Vulcan carbon acted as the growth support. Previous studies on using various supports for use in oxygen reduction catalysts has been conducted [11-13]. The magnesia and Vulcan carbon supports were selected based on having high ORR activities. The study of higher iron loadings in these supports will provide information as to whether or not higher iron content helps or inhibits catalyst activity.

In addition to the use of two growth supports, the metal loading applied during IWI was varied. The metal loadings investigated are 6, 10, and 15 weight percent. Table 1 below provides a list of the catalysts investigated in this thesis.

**Table 1: Metal Loadings of Catalysts Prepared**

<b>Catalyst Support</b>	<b>Iron Loading (Wt Percentage)</b>
Magnesium Oxide (HSA)	6
Magnesium Oxide (HSA)	10
Magnesium Oxide (HSA)	15
Vulcan Carbon	6
Vulcan Carbon	10
Vulcan Carbon	15

This thesis will investigate the activity and/or selectivity of the oxygen reduction catalysts that are formed during the decomposition of acetonitrile growth medias listed in Table 1. In addition, XANES analysis of the iron K-edge in the ORR catalysts will

provide information on the composition and unoccupied electronic states of iron within the catalysts.

### *Catalysts Grown over Magnesium Oxide Supports*

Activity tests using the RDE were performed on the catalysts grown over the magnesia support. The ORR activity data collected indicates the higher metal loadings have slower onsets of activity; this trend can be seen in Figure 4.

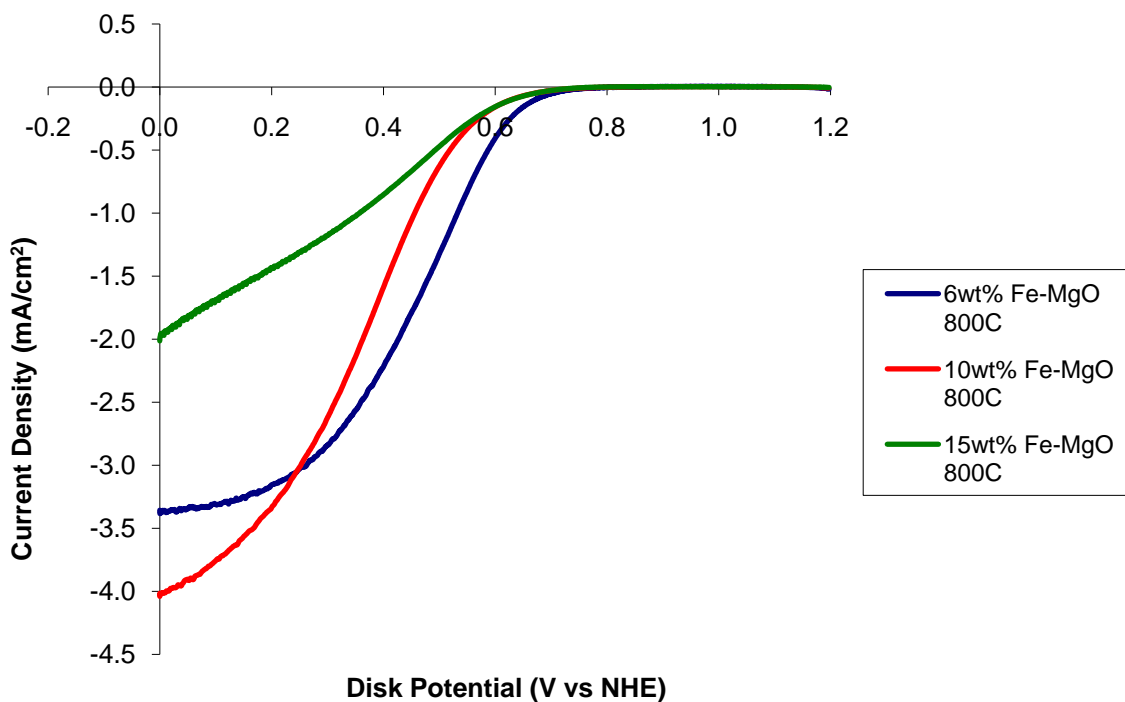


Figure 4: RDE Activity Comparison of Iron Metal Loading in Catalysts Prepared Using MgO Support

The onset of activity is defined as the point when the cathode reduction current obtained in an oxygen-saturated environment increases relative to the collected argon background scan. For RDE, this point is found when the current density in the disk is one percent greater than the argon background collected. Figure 4 clearly shows that the 6 weight

percent catalyst diverges first, indicating that the catalyst is initially more active than the 10 weight percent and 15 weight percent catalysts. However, the graph also displays an interesting discovery that is contrary to the initial hypothesis, which anticipated decreased activity of the catalysts with increased metal loading. The experiments found that the 10 weight percent catalyst had the greatest peak current density at  $4.02 \text{ mV/cm}^2$ , while the 6 weight percent catalysts had a lower peak current density of  $3.36 \text{ mV/cm}^2$ . This finding, though not predicted, could be the result of an anomaly and requires further investigation and verification.

In addition to the RDE testing, RRDE tests were conducted on the three Fe-MgO catalysts. RRDE testing allows for the study of not only a catalysts activity, but also the selectivity of the catalyst. The ORR selectivity is defined as the average number of electrons transferred from one oxygen molecule at the disk over a range of potentials [11]. Based on the aforementioned reactions that occur during oxygen reduction, a selectivity value of 4.0 is desired because this represents the complete reduction of oxygen to water. On the other hand, a selectivity value of 2.0 is undesirable because this indicates a partial reduction of oxygen to hydrogen peroxide. The formation of hydrogen peroxide will cause irreversible damage to fuel cell components because it is a strong oxidant and overtime reduce the fuel cell performance. All the catalysts grown over the magnesia support displayed selectivities within the normal range of 3.6 to 4.0. Furthermore, the RRDE activities found indicate the same result as the RDE test and are shown in Figure 5.

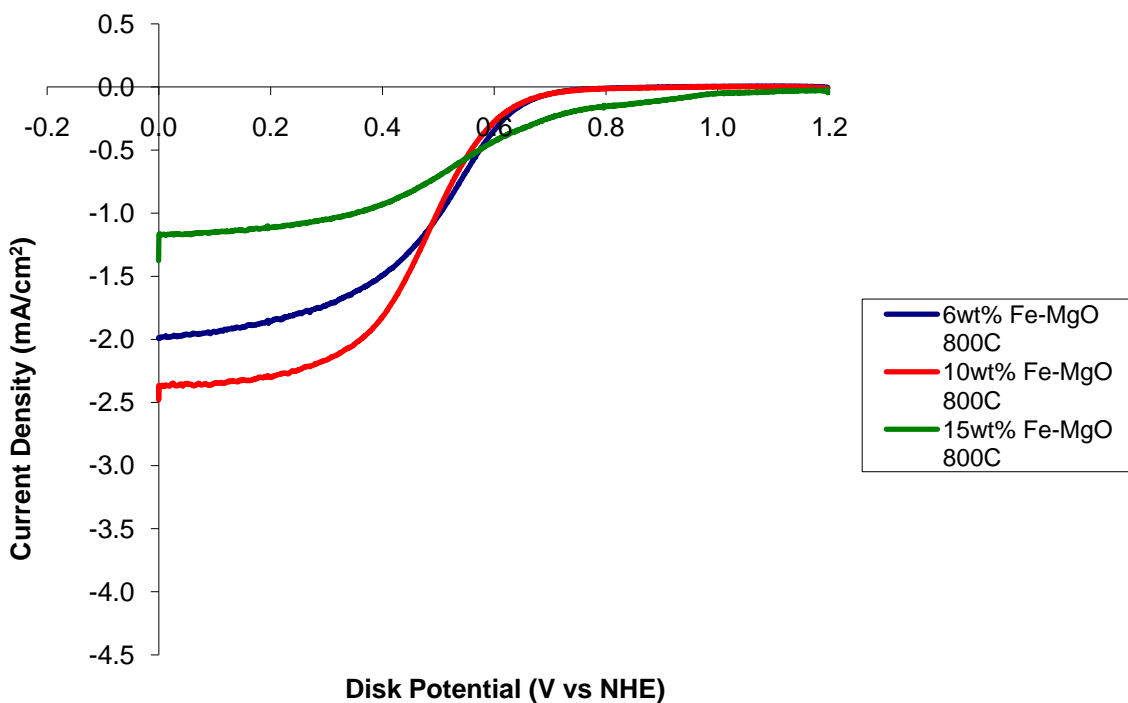


Figure 5: RRDE Activity Comparison of Iron Metal Loading in Catalysts Prepared Using MgO Support

Once again, the hypothesis that higher metal loading will decrease the activity of the catalyst is not indicated by the graph above. However, the same catalysts tested on the RDE were tested on the RRDE, which is an indication of consistency in the results.

In order to better understand local bonding environment of these higher metal loading catalysts, XANES testing was conducted. The background-subtracted complete absorption spectra of 6 weight percent Fe-MgO IWI precursor obtained at room temperature under the flow of nitrogen, at 800°C, and under the flow of acetonitrile at 800°C, respectively can be viewed in Figure 6. The data collected at room temperature was the least noisy, and it became noisier at higher temperatures with the same artifacts appearing for both the data sets at 800°C under nitrogen flow and 800°C under

acetonitrile flow. This can be attributed to the increase in the intermolecular interactions in the sample at higher temperatures due to increased kinetic energies.

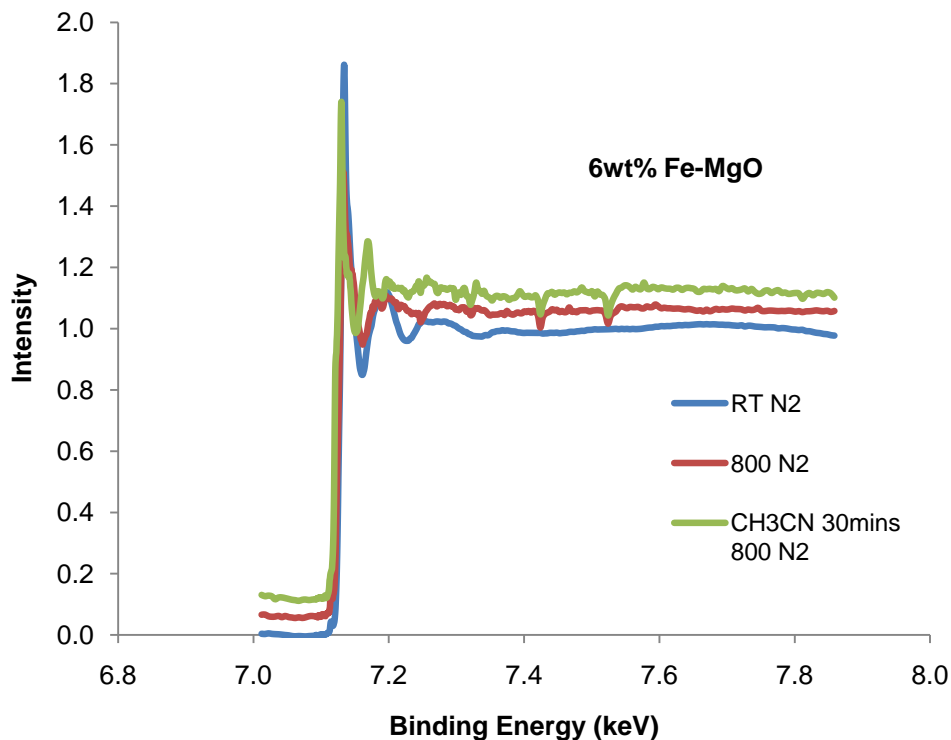


Figure 6: Complete Absorption Spectra of 6 weight percent Fe-MgO  
Data Collected By Deepika Singh

Data fitting with the standards mentioned above ( $\text{Fe}_2\text{O}_3$ ,  $\text{FeO}$ ,  $\text{Fe}_3\text{O}_4$ ,  $\text{FeC}$ , and pure Fe foil) was also conducted and the results can be seen in Figure 7. At room temperature, the iron acetate-impregnated MgO support chiefly consisted of Fe in the form  $\text{Fe}_3\text{O}_4$ . There was considerable difficulty encountered in obtaining exact fits, due to the presence of mixed oxides of iron along with magnesia. At  $800^\circ\text{C}$  under nitrogen flow, the sample formed a more discernible separate mixture of  $\text{FeO}$  and  $\text{Fe}_2\text{O}_3$ . Whereas in the reducing environment of 30 minutes of acetonitrile flow, the sample reduced to form mostly metallic iron and iron carbide, due to carbon growth occurring at these temperatures, when the sample is exposed to a carbon source. Upon analysis of data

collected at 60, 90 and 120 minutes of acetonitrile flow, there were no differences observed in the spectra, they were essentially the same as the one obtained at 30 minutes of acetonitrile flow. This phenomenon could possibly be due to the growth of carbon nanostructures on the surface of the pellet, and all the acetonitrile in the carrier gas would be exhausted before reaching the bulk of the pellet. Since EXAFS/XANES is a bulk technique, there was no change in the iron phase observed after the initial growth of carbon set in.

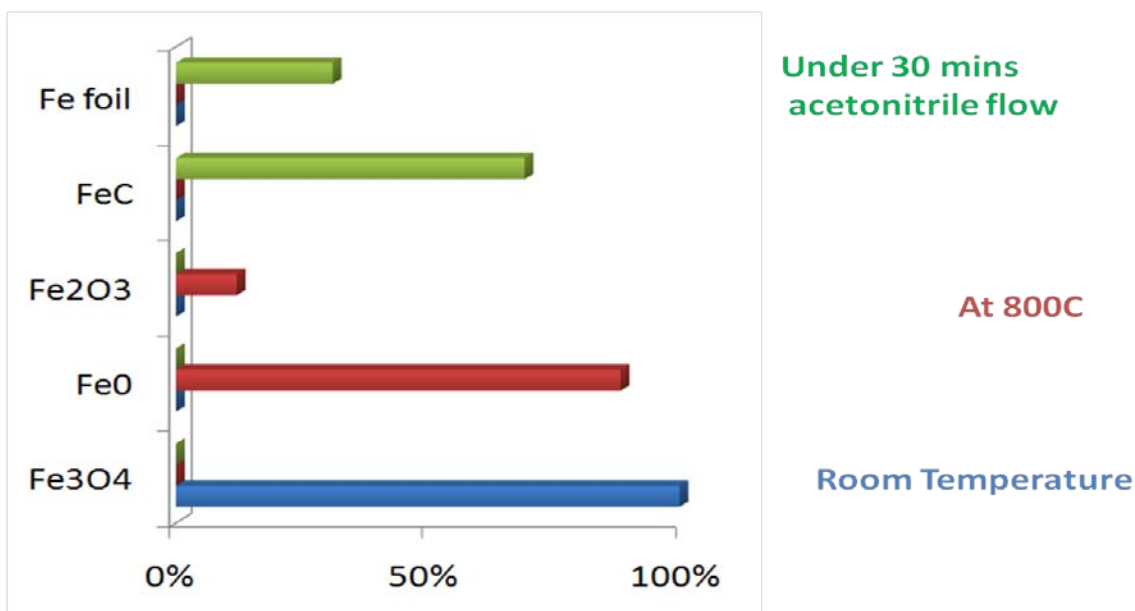
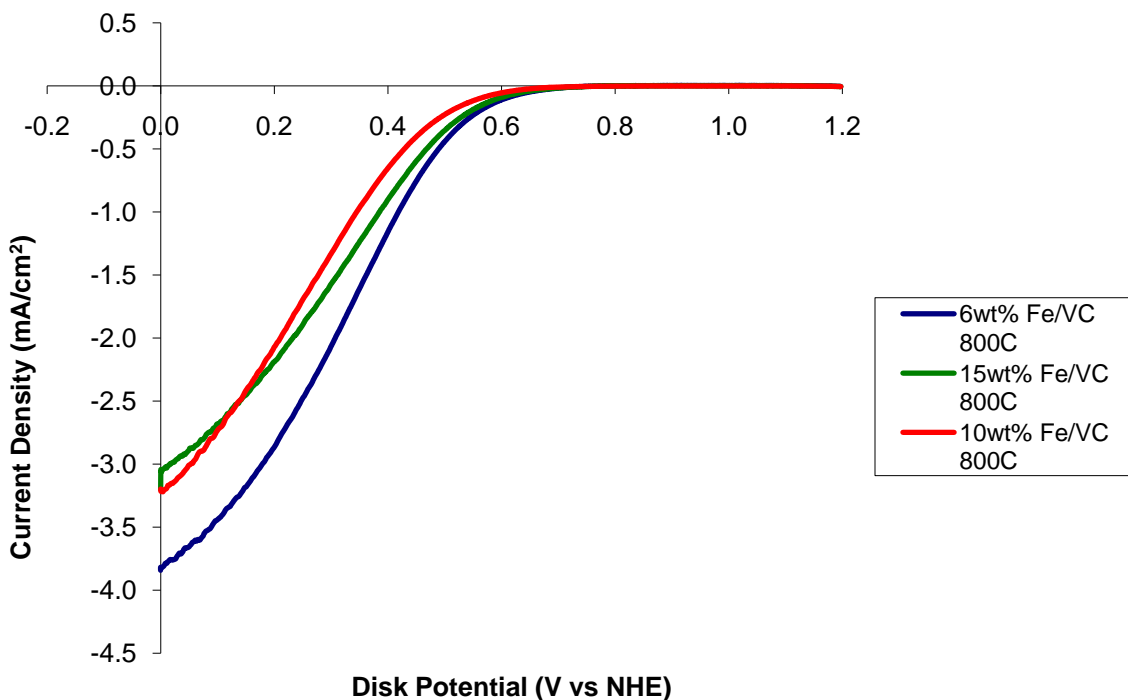


Figure 7: Percentage composition of Fe<sub>2</sub>O<sub>3</sub>, FeO, Fe<sub>3</sub>O<sub>4</sub>, FeC, and pure Fe foil in MgO samples  
Data Collected By Deepika Singh

### *Catalysts Grown over Vulcan Carbon Supports*

Activity tests using the RDE were performed on the catalysts grown over Vulcan carbon support. The ORR activity data collected indicates the same trend that was observed for the catalysts grown over magnesia support. The higher iron metal loadings yielded slower onsets of activity; this trend is shown in Figure 8.





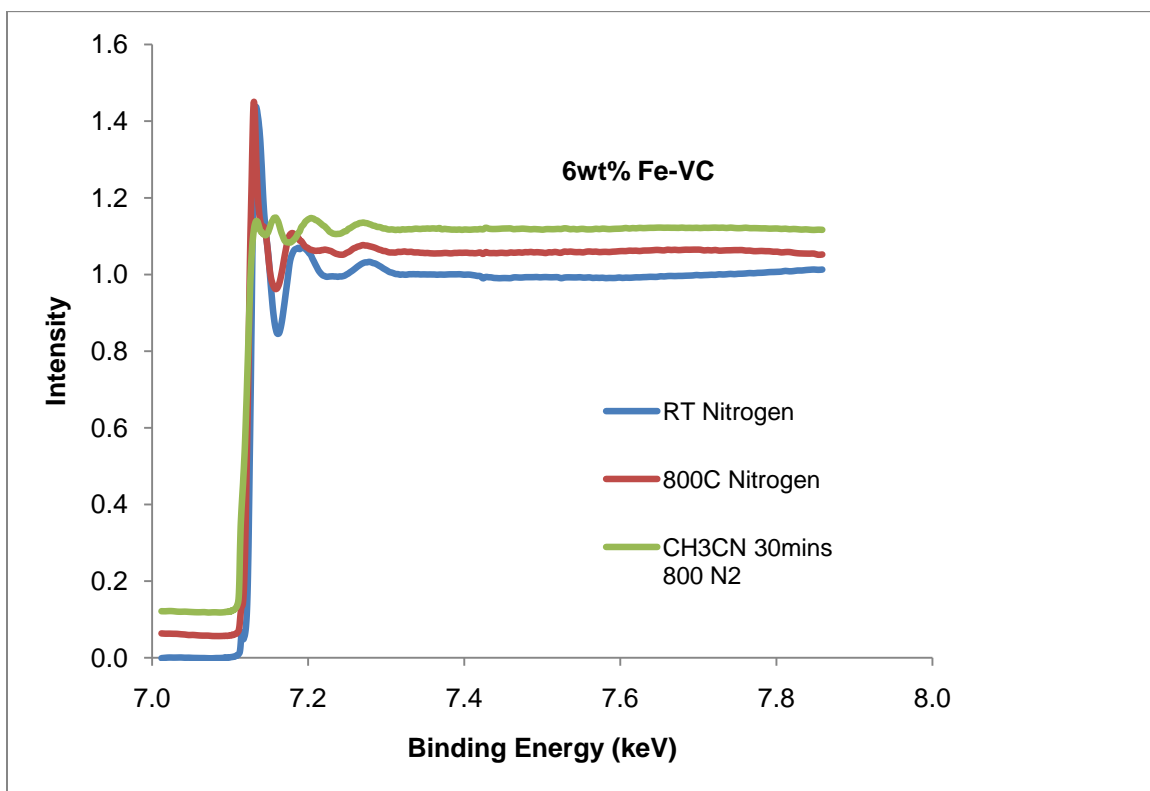
**Figure 8: RDE Activity Comparison of Iron Metal Loading in Catalysts Prepared Using VC Support**

Figure 8 clearly shows that the 6 weight percent catalyst diverges first, indicating that the catalyst is initially more active than the 10 weight percent and 15 weight percent catalysts. The hypothesis that higher metal loadings have lower activity is supported by this RDE study of the catalysts grown over Vulcan carbon. The 6 weight percent catalyst has a peak current density of 3.84 mV/cm<sup>2</sup>. While the 10 weight percent and 15 weight percent catalysts have peak current densities of 3.21 mV/cm<sup>2</sup> and 3.19 mV/cm<sup>2</sup> respectively.

One theory that may explain why higher iron loading catalysts have lower activity is that iron tends to agglomerate together when heated to high temperatures, thus leading to blockage of active sites. However, to better understand the reason for higher iron

loadings decrease in activity, more information is needed on the active site of the catalysts.

In an attempt to further understand the effect higher metal loading has on CNx catalyst, XANES testing was conducted. Vulcan carbon impregnated with 6 weight percent iron acetate, showed differences in the observed spectra collected at room temperature, at 800°C and under 30 minutes of acetonitrile flow at 800°C, which can be seen in Figure 9.



**Figure 9: Complete Absorption Spectra of 6 weight percent Fe-VC  
Data Collected By Deepika Singh**

Data fitting with the standards results can be viewed in Figure 10. Room temperature XANES data demonstrated a higher concentration of a lower oxide, i.e.,  $\text{Fe}_2\text{O}_3$  and around 8% of mixed oxides of iron in the form of  $\text{Fe}_3\text{O}_4$ . At 800°C under the flow of nitrogen, iron was primarily present in the +2-oxidation state as  $\text{FeO}$ . Under

acetonitrile flow, iron was reduced further to metallic iron and iron carbide, again due to carbon growth. These results are coherent with previously acquired Mossbauer data obtained on iron-57 enriched sample in our research group, where  $\text{Fe}_3\text{C}$  was found to be the dominant phase in pyrolyzed and 1M HCl washed  $\text{CN}_x$ .

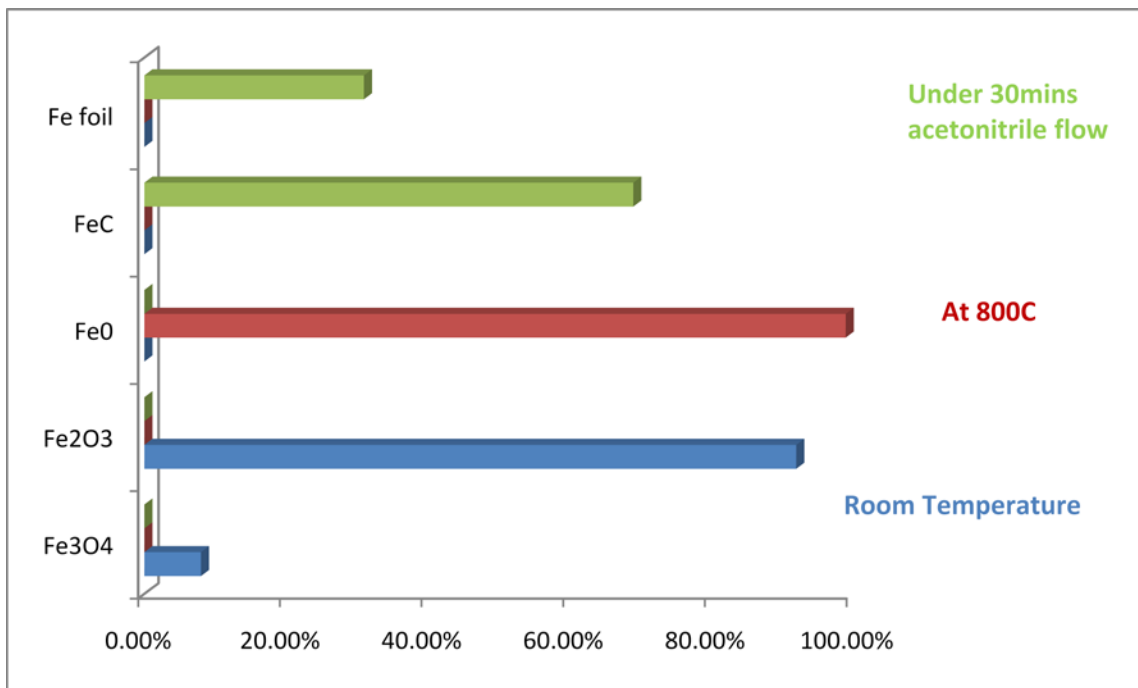


**Figure 10: Percentage composition of  $\text{Fe}_2\text{O}_3$ ,  $\text{FeO}$ ,  $\text{Fe}_3\text{O}_4$ ,  $\text{FeC}$ , and pure Fe foil in VC sample  
Data Collected By Deepika Singh**

The higher metal loading catalysts pyrolyzed in-situ while collecting X-Ray spectra yielded similar differences between the room temperature, 800°C and acetonitrile-flow scans. However, further analysis of EXAFS data is required to observe subtle differences in the particle size, and coordination states of iron in higher loading catalysts.

## CONCLUSIONS

CN<sub>x</sub> catalysts were prepared using two growth supports and various iron metal loadings. Although all the catalysts were still active for ORR, two general trends were found. The trends indicate that higher metal loading catalysts are slower to reach initial activity and as a result achieve lower peak current densities. Information on the effect iron has in oxygen reduction catalysts can provide further insight into the reaction that is occurring at the cathode of a fuel cell and allow for optimization of the catalysts to occur, making PEM fuel cells a more marketable device.

XANES analysis of 6 weight percent iron on two different supports, magnesia and Vulcan carbon, showed differences in the oxidation states of iron at different stages of pyrolysis. Since iron is present mostly in the form of iron carbide (or possibly coordinated to other lighter elements such as nitrogen) and metallic iron, it is most likely that iron is present in this state while initiating carbon growth on the conductive support, which would then be active for ORR once the support and iron is washed away subsequent to acid wash. The XANES spectra for 10 weight percent and 15 weight percent Fe-MgO and Fe on VC were similar to the one obtained for 6 weight percent Fe-MgO. This could be attributed to the increased concentration of iron being in the bulk phase, which was not affected by the acetonitrile-enriched nitrogen flowing through the sample, since most of the acetonitrile would be consumed for the growth of carbon on the surface of the sample. Further EXAFS analysis of these samples would yield significant insight into its coordination states and local bonding environments.

## **FUTURE WORK**

Additional data analysis and catalyst characterization is required to verify the findings of this thesis. More activity and selectivity data should be acquired for multiple catalysts that contain higher iron loadings to enable rigorous statistical analysis of the data to be conducted. The conclusions from statistical analysis can then establish if a significant difference exists between the activities of higher metal loading catalysts. Additional investigation of the catalyst surface features and composition should also be conducted using techniques such as transmission electron microscopy imaging to determine the morphology of the carbon nanostructures formed and X-Ray diffraction to characterize the phase and size of the iron nanoparticles within  $\text{CN}_x$  and the degree of graphite character of the carbon. Further work with higher metal loading non-precious metal catalysts may provide insight into the role of iron in ORR catalyst active sites.

## LIST OF REFERENCES

- [1] Matter, Paul H., Ling Zhang, and Umit S. Ozkan. "The Role of Nanostructure in Nitrogen-containing Carbon Catalysts for the Oxygen Reduction Reaction." *Journal of Catalysis* 239 (2006): 83-96. Print.
- [2] Jasinski, Raymond. "A New Fuel Cell Cathode Catalyst." *Nature* 201.4925 (1964): 1212-213.
- [3] Jasinski, Raymond. "Cobalt Phthalocyanine as a Fuel Cell Cathode." *Journal of the Electrochemical Society* 112.5 (1965): 526-28.
- [4] Yeager, Ernest. "Electrocatalysis for O<sub>2</sub> Reduction." *Electrochimica Acta* 9.11 (1984): 1527-537.
- [5] Yeager, Ernest. "Dioxygen Electrolysis: Mechanisms in Relation to Catalyst Structure." *Journal of Molecular Catalysis* 38 (1986): 5-25.
- [6] Lalande, G. "Is Nitrogen Important in the Formulation of Fe-based Catalysts for Oxygen Reduction in Solid Polymer Fuel Cells?" *Electrochimica Acta* 42.9 (1997): 1379-388.
- [7] Bezerra, C., L. Zhang, K. Lee, H. Liu, A. Marques, E. Marques, H. Wang, and J. Zhang. "A Review of Fe–N/C and Co–N/C Catalysts for the Oxygen Reduction Reaction." *Electrochimica Acta* 53.15 (2008): 4937-951.
- [8] Gasteiger, Hubert A., and Nenad M. Markovic. "Just a Dream-or Future Reality?" *Science Magazine*. AAAS, 3 Apr. 2009.

- [9] Lefevre, M., J. P. Dodelet, and P. Bertrand. "O<sub>2</sub> Reduction in PEM Fuel Cells: Activity and Active Site Structural Information for Catalysts Obtained by the Pyrolysis at High Temperature of Fe Precursors." *J. Phys. Chem. B* 104 (2000): 11238-1247.
- [10] Shao, Yuyan, Jiehe Sui, Geping Yin, and Yunzhi Gao. "Nitrogen-doped Carbon Nanostructures and Their Composites as Catalytic Materials for Proton Exchange Membrane Fuel Cell." *Applied Catalysis B: Environmental* 79.1 (2008): 89-99.
- [11] Biddinger, Elizabeth J., Dieter Von Deak, and Umit S. Ozkan. "Nitrogen-Containing Carbon Nanostructures as Oxygen-Reduction Catalysts." *Top Catal* 52 (2009): 1566-574.
- [12] Matter, P., E. Wang, and U. Ozkan. "Preparation of Nanostructured Nitrogen-containing Carbon Catalysts for the Oxygen Reduction Reaction from SiO<sub>2</sub>- and MgO-supported Metal Particles." *Journal of Catalysis* 243.2 (2006): 395-403.
- [13] Matter, Paul H., Eugenia Wang, Jean-Marc M. Millet, and Umit S. Ozkan. "Characterization of the Iron Phase in CN<sub>x</sub>-Based Oxygen Reduction Reaction Catalysts." *Journal of Physical Chemistry C* 111.3 (2007): 1444-450.
- [14] Cote, R., G. Lalande, G. Faubert, D. Guay, J. P. Dodelet, and G. Denes. "Non-noble Metal-based Catalysts for the Reduction of Oxygen in Polymer Electrolyte Fuel Cells." *Journal of New Materials for Electrochemical Systems* 1 (1998): 7-16.
- [15] Biddinger, Elizabeth J., Dieter Von Deak, Deepika Singh, Hilary Marsh, Bing Tan, Douglas S. Knapke, and Umit S. Ozkan. "Examination of Catalyst Loading Effects on the Selectivity of CN<sub>x</sub> and Pt/VC ORR Catalysts Using RRDE." *Journal of The Electrochemical Society* 158.4 (2011): B402-B409.